Proceedings of Anticancer Research, 2023, Volume 7, Issue 4
http://ojs.bbwpublisher.com/index.php/PAR
ISSN Online: 2208-3553
ISSN Print: 2208-3545

Biosynthesis and Characterization of Silver Nanoparticles Coated with Metabolites Extracted from *Clerodendron phlomoides* with Its Biochemical Studies in Liver Tissue

Subha Veeramani[1], Kirubanandan Shanmugam[2]*

[1]National Centre for Nanoscience and Nanotechnology, University of Madras, Chennai 600025, India

[2]Saveetha School of Engineering, Saveetha Institute of Medical and Technical Sciences (SIMATS), Thandalam, Chennai 602105, India

***Corresponding author:** Kirubanandan Shanmugam, kirubanandan.shanmugam@gmail.com

Abstract: Silver nanoparticles (AgNPs) have been used as a potential nanomaterial-based drug delivery vehicle for liver cancer treatment, as it induces cell death and produces cytotoxicity against cancerous cells at a low concentration. The biosynthesis of green metallic nanoparticles uses secondary metabolites in plant extracts instead of toxic chemicals for a reduction-oxidation (redox) reaction. The biosynthesis of AgNPs with the aqueous extract of *Clerodendron phlomoides* was performed in this study. The phytochemical analysis of *C. phlomoides* extract using gas chromatography-mass spectrometry (GC-MS) confirmed the presence of redox metabolites. The peak at 489 nm in UV-visible spectra confirmed the formation of bioactive AgNPs reduced from silver nitrate solution, whereas the Fourier-transform infrared (FTIR) spectra indicated the bioactive molecules of plant extracts that are responsible for the formation. Scanning electron microscope (SEM) micrograph revealed the formation of spherical and ovoid structures of AgNPs, whereas transmission electron microscope (TEM) micrograph confirmed the size of AgNPs, which varies from 25 nm to 100 nm. X-ray diffraction (XRD) spectra showed the crystalline nature of AgNPs, and the size of crystallite was 4 nm, while dynamic light scattering (DLS) analysis confirmed the average particle size of AgNPs to be around 125 nm. *In vivo* studies showed that bioactive AgNPs have a significant anticancer potential against liver cancer, whereas biochemical studies of rats' liver tissue samples confirmed that bioactive AgNPs produced a potential hepatoprotective effect against diethylnitrosamine-induced liver cancer.

Keywords: Silver nanoparticles; *Clerodendron phlomoides*; Aqueous extract; SEM; TEM; Liver cancer

Online publication: July 05, 2023

1. Introduction

One of the most important organs is the liver and it functions mainly for various metabolism involved in the body. It predominantly works for glucose homeostasis, storage of vitamins and minerals, lipid synthesis and metabolism, maintenance of excess amino acids, ammonia, and bile production [1]. Apart from these functions, the liver plays a major role in the detoxification and metabolism of toxic and xenobiotics and produces enzymes such as cytochrome P450 (CYP 450). This enzyme converts toxic chemicals into hydrophilic substances for easy excretion in the urine via metabolism [2]. Hepatocellular carcinoma (HCC) is a form of liver cancer that is caused by genetic alterations, albeit the progression of HCC remains obscure

in the pathophysiology. The predicted genetic alterations for HCC included mutations, amplifications, and deletions in genomic aspects, as well as epigenetic alterations such as abnormal changes in methylation patterns [3]. HCC has a high metastatic potential and confrontation with contemporary therapeutic approaches that is the most challenging in the field of clinical oncology [4]. Therefore, there is a critical requirement for developing new therapeutic drugs and more efficient site/target-specific drug delivery vehicles [4].

In past decades, metallic nanoparticles have played an important role in medicine for the treatment of various ailments, such as cancer [5]. Precious metal nanoparticles have notable properties, such as excellent biocompatibility, stability, and photostability. In addition to that, metallic nanostructures have favorable physical, chemical, and biological properties as well as functionality in view of their nanoscale size [6,7]. Silver and its oxide nanoparticles (AgNPs) are the predominant metallic nanomaterials used for various functional applications [8]. It has considerable properties such as catalytic, optical, and antimicrobial properties. AgNPs play a predominant role as potential antimicrobial bionanomaterials against various microorganisms and pathogens. Through various mechanisms such as cell membrane breakage and penetration, silver ion in AgNPs eradicates and combats pathogens effectively [9].

AgNPs have not only a bacteriostatic and chemotherapeutic effect but also the capacity for inducing apoptosis in cancerous cells [10,11]. The reported mechanism of AgNPs-induced cell apoptosis is the cleavage of double-strand DNA, follow by oxidative stress production via the formation of free radicals, leading to the instability of chromosomes [12]. The size of AgNPs is one of the biggest advantages in producing anticancer potential against cancerous cells. Smaller nanoparticles penetrate the cancerous cells much more efficiently as compared to larger particles and interact with the nucleus by delivering either the anticancer agents or the biotherapeutic agents and producing more cytotoxic against the cancerous cells. Hence AgNPs can be used as a base biomaterial for the fabrication of drug targeting and delivery into the cells [13]. AgNPs also contribute as diagnostic agents, image contrast agents, and also biosensors to achieve the specific imaging process in biomedical applications. A recent study also showed that AgNPs can be used as chemotherapeutic material for the treatment of diethylnitrosamine (DEN)-induced liver cancer and gives hepatoprotective activity to the liver cells against DEN toxicity [14].

Numerous investigations on silver nanoparticle synthesis were reported. However, the chemical and physical methods for the synthesis of AgNPs have several limitations in the formation of nanoparticles, as there was consumption of toxic and expensive chemicals. To eliminate these limitations, green synthesis of silver nanoparticles via plant extract promotes the reduction and oxidation (redox) of silver nitrate solution into silver nanoparticles. The plant extract consists of various secondary metabolites functioning as agents for redox reactions leading to the formation of nanoparticles. Furthermore, these secondary metabolites make nanoparticles bioactive via coating nanoparticles [15].

Clerodendrum phlomidis Linn is a well-known medicinal plant used in Traditional practice and culture, and its leaves have been used in Ayurvedic and Siddha Medicine. This plant medicine was used for the treatment of inflammation, diabetes, nervous disorder, asthma, rheumatism, digestive disorders, urinary infection and disorders, and bitter tonic. The alcoholic and aqueous extract of the leaves has properties such as analgesic, anti-diarrheal, anti-plasmodial, hypoglycemic, minor tranquilizers, anti-asthmatic, anti-fungal, nematicidal, anti-amnestic, and anti-arthritic. Therefore, it was considered a material used for the green synthesis of nanoparticles considering its wide therapeutic potential [16].

This paper investigated the anticancer potential of silver nanoparticles against liver cancer induced in albino rats and biochemical studies of tissue taken from the liver treated by silver nanoparticles. The silver nanoparticles will be synthesized via a green synthetic approach with the extract from the leaves of *Clerodendrum phlomidis Linn*, hereby known as *C. phlomidis*.

2. Materials and methods

Analytical grade chemicals were supplied by Merck Sigma-Aldrich (USA), HiMedia Laboratories (India), and S.D. Fine Chem Ltd. (India), and were used throughout this scientific work. Silver nitrate (AR Grade) was the major precursor used in the synthesis of silver nanoparticles (AgNPs).

2.1. Plant extract preparation:

Five grams of *C. phlomidis* dried leaves were well grounded and soaked in 100 ml of the double-distilled water for 3 hours and then boiled for 30 min at a temperature of 100 ± 5°C until the solution turned completely brownish and turbid with crude plant extract. The given solution was cooled down to room temperature of nearly 15°C to 20°C, followed by filtered with Whatman 1 filter paper for the collection of the resultant filtrate, which contained the potential secondary metabolites and various bioactive molecules. This filtrate was then stored in a cold room at a temperature of 4°C for further use in the biosynthesis of silver nanoparticles.

2.2. Biosynthesis of silver nanoparticles

One millimolar of silver nitrate (Sigma AR Grade) was dissolved in 100 mL of double-distilled water and then added to 10 mL of an aqueous plant extract. The whole mixture was mixed under continuous stirring at 70 rpm. This experiment was carried out at a temperature of 50°C and a pH of 7 was maintained. Synthesized silver nanoparticles were centrifugated at 12,000 rpm. The freeze-dried silver nanoparticles were performed by a lyophilizer and the dried AgNPs were used for particle size analysis, morphological and topographical analyses, X-ray diffraction (XRD) studies, and zeta potential studies. The dried silver nanoparticles were used for anticancer activity studies against DEN-induced liver toxicity in albino rats.

2.3. Analysis of plant extract using gas chromatography-mass spectrometry

The given plant extracts were subjected to phytochemical analysis via gas chromatography-mass spectrometer (GC-MS), which evaluates the identification of the types of secondary metabolites. Perkin Elmer Auto System XL GC-MS analyzer was used, where 70 eV has been used for electron ionization energy for GC-MS analysis, and helium gas was used as a mobile gas phase and carrier. Helium was used at a flow rate of 1.51 mL/min with a plant extract sample load of 2 µL. Total GC-MS running time was 22 min. TurboMass software was used to analyze the chromatogram of the plant extracts. Identification of the compounds was carried out with the support of a database in the National Institute of Standards and Technology (NIST).

2.4. UV-visible spectroscopy studies of silver nanoparticles

Ten milliliters of plant extract were mixed with 1 mM $AgNO_3$ solution to synthesize bioactive nanoparticles. The formation of AgNPs was confirmed as the solution changed to brown color within 30 minutes. The plant extract contains plant flavonoids that can reduce $AgNO_3$ into silver nanoparticles. The size, shape, concentration, and agglomeration of AgNPs were investigated using UV-visible (UV-vis) spectrophotometer. The comparison between the free nanoparticles and agglomerated nanoparticles was investigated by studying the surface plasmon resonance (SPR) absorption band. For the agglomerated silver nanoparticles, the absorption band shifts to red (longer wavelength) as compared to the absorption band of free silver nanoparticles.

2.5. Scanning electron microscopy of silver nanoparticles

The morphology and shape of the AgNPs were evaluated using scanning electron microscopy (SEM) JEOL JSM IT1800. Dried AgNPs were subjected to SEM evaluation for analysis of the surface topography of the

nanoparticle. The carbon tape was stuck on the metallic stub and then a small quantity of AgNPs was added to the carbon tape and spread well on the area 5 × 5 mm. Nitrogen was then sprayed on the sample on the stub to remove any free nanoparticles. The images are taken in secondary electron mode in an SEM instrument and the SEM micrographs are captured at 5 microns.

2.6. Transmission electron microscopy of silver nanoparticles

The shape and topography of the silver nanoparticles were evaluated using transmission electron microscopy (TEM), which can be interpreted for anticancer activity. A drop of AgNPs suspension was taken on the copper grid and dried before image capture. The TEM micrographs were captured for the analysis of the size and shape of AgNPs.

2.7. Fourier-transform infrared spectroscopy studies of silver nanoparticles and secondary metabolites:

The silver nanoparticles coated by the secondary metabolites were analyzed using Fourier-transform infrared (FTIR) spectroscopy. In this analysis, the functional groups of secondary metabolites in the plant extract and then coated on the silver nanoparticles are investigated with FTIR spectra. The functional groups in the plant extract responsible for the reduction of silver nitrate into silver nanoparticles were also analyzed using FTIR RX1-Perkin Elmer in the wavelength range 4000-400 cm^{-1}.

2.8. X-ray diffraction analysis

The crystalline nature of biosynthesized silver nanoparticles was evaluated using X-ray diffraction (XRD) analysis with XPERT-PRO using monochromatic Cu kα radiation (λ = 1.5406 Å) operated at 40 kV and 30 mA at a 2θ angle pattern, and the scanning was performed in the region from 20° to 80°. The collected data were analyzed with the support of the Joint Committee on Powder Diffraction Standards (JCPDS) library to account for the crystalline structure of silver nanoparticles.

2.9. Dynamic light scattering analysis

The size distribution and stability of biosynthesized nanoparticles were investigated using a dynamic light scattering (DLS) instrument from Malvern Panalytical. The zeta potential of AgNPs was also determined by this measurement.

2.10. *In vivo* studies for evaluation of the anticancer potential of metallic nanoparticles

The biochemical studies of the anticancer potential of AgNPs were investigated via animal studies using Wister albino rats. Group 1 is considered the control group where the rats were fed with standard rat chow and pure drinking water *ad libitum.* For Groups 2–6, the rats were induced with liver carcinogenesis via intra-peritoneal injection of DEN (25 mg/kg body weight) in a single administration. DEN was dissolved in 0.5 mL of sterile water. In Group 3, the DEN-induced rats were treated with AgNPs to evaluate the anticancer potential of nanoparticles. The oral administration of AgNPs with a concentration of 10 mg/kg body weight was fed into the rats daily for 30 days. Group 4 DEN-induced rats were treated with selenium nanoparticles (SeNPs), group 5 DEN-induced rats were treated with palladium nanoparticles (PdNPs), and group 6 DEN-induced rats were treated with plant extracts.

3. Results and discussion

The phytochemical analysis of the plant extract was evaluated via GC-MS and chemical methods to evaluate the type of secondary metabolites in the extract. These secondary metabolites play a major role in the synthesis of silver nanoparticles and also coat the nanoparticles to achieve biological activity and

produce therapeutic effects such as anticancer potential against cancerous cells in the DEN-induced liver. In addition to that, these secondary metabolites act as redox agents in the biosynthesis of silver nanoparticles in an eco-friendly approach without any harmful products. These secondary metabolites increase the synergistic mechanism of AgNPs via coating the nanoparticles. As a result, the therapeutic effect of the biosynthesized nanoparticles was enhanced [17].

3.1. Phytochemical analysis

Aqueous extract of *C. phlomoides* was tested for their phytochemical constituents using various qualitative assays. In this study, alkaloids, flavonoids, phenols, glycosides, carbohydrates, and terpenoids were found in the aqueous extract of *C. phlomoides.* The results obtained were tabulated in **Table 1** stating that glycosides were present in leaves extract of *C. phlomoides*; flavonoids and alkaloids were present in all parts of the plant. The aqueous leaves extract showed positive for several phytoconstituents and the active constituents act as redox agents for the synthesis of silver nanoparticles.

Table 1. GC-MS data of *C. phlomoides* plant aqueous leaves extract

Chemical compounds	RT	Area	Molecular formulae	Molecular Weight	Compounds
2-Hexadecen-1-ol,3,7,11,15-tetramethyl-,[R-[R*,R*-(E)]]-(CAS)Phytol	33.790	1.40	$C_{20}H_{40}O$	296	Acyclic diterpene alcohol
9,12,15-Octadecatrienoic acid, methyl ester,(Z,Z,Z)-(CAS)Methyl linolenate	37.058	12.39	$C_{19}H_{32}O_2$	292	-
Naringenin	24.032	19.50	$C_{15}H_{12}O_5$	272.068	Polyphenolic compounds
6-Methoxy apigenin (Hispidulin)		19.50	$C_{16}H_{12}O_6$		
α-terpinene	C	0.03	$C_{10}H_8O_3$	136	Terpenoid
1,2,3-Propanetriol (CAS) Glycerol	10.332	2.29	$C_3H_8O_3$	92	Polyol
Geranyl Linalool isomer	38.757	4.68	$C_{20}H_{34}O$	290	Terpenoids
4H-Pyran-4-one, 2,3-dihydro-3,5-dihydroxy-6-methyl	33.142	0.59	$C_6H_8O_4$	144	Flavonoid Fraction
Quercetin	17.17	19.50	CHO	270	Flavonoids
1,2,3-Propanetriol (CAS) Glycerol	10.332	2.29	$C_3H_8O_3$	92	Polyol
Ethyl iso-allocholate	35.367	0.06	$C_{26}H_{44}O_5$	436	Steroid

Table 2 summarizes the presence of the various secondary metabolites in an aqueous plant extract and these metabolites coated on the silver nanoparticles. Carbohydrates, alkaloids, flavonoids, and terpenoids are present on the AgNPs via coating while synthesizing the nanoparticle. These secondary metabolites present on the silver nanoparticles produce anticancer activity against liver cancer that not only targets directly the cancerous cell in the liver but also synergistically produces a therapeutic effect against the cancer cell.

Table 2. Phytochemical analysis of *C. phlomoides* plant aqueous leaves extract and AgNPs

Phytochemical	Plant extract	AgNPs
Carbohydrates	+	+

(Continued on next page)

(Continued from previous page)

Phytochemical	Plant extract	AgNPs
Glycosides	+	-
Alkaloids	+++	++
Flavonoids	+	+
Steroids	+	-
Tannins	+	-
Saponins	+	-
Terpenoids	+	-
Polyphenols	+	+

Figures 1 and **2** show the GC-MS of *C. phlomoides* plant aqueous leaves extract. The spectra confirmed the presence of various secondary metabolites with the elucidated structure of the compounds in the extract. These compounds can produce various pharmacological effects with silver nanoparticles. As discussed earlier, these compounds also act as redox agents for the synthesis of silver nanoparticles.

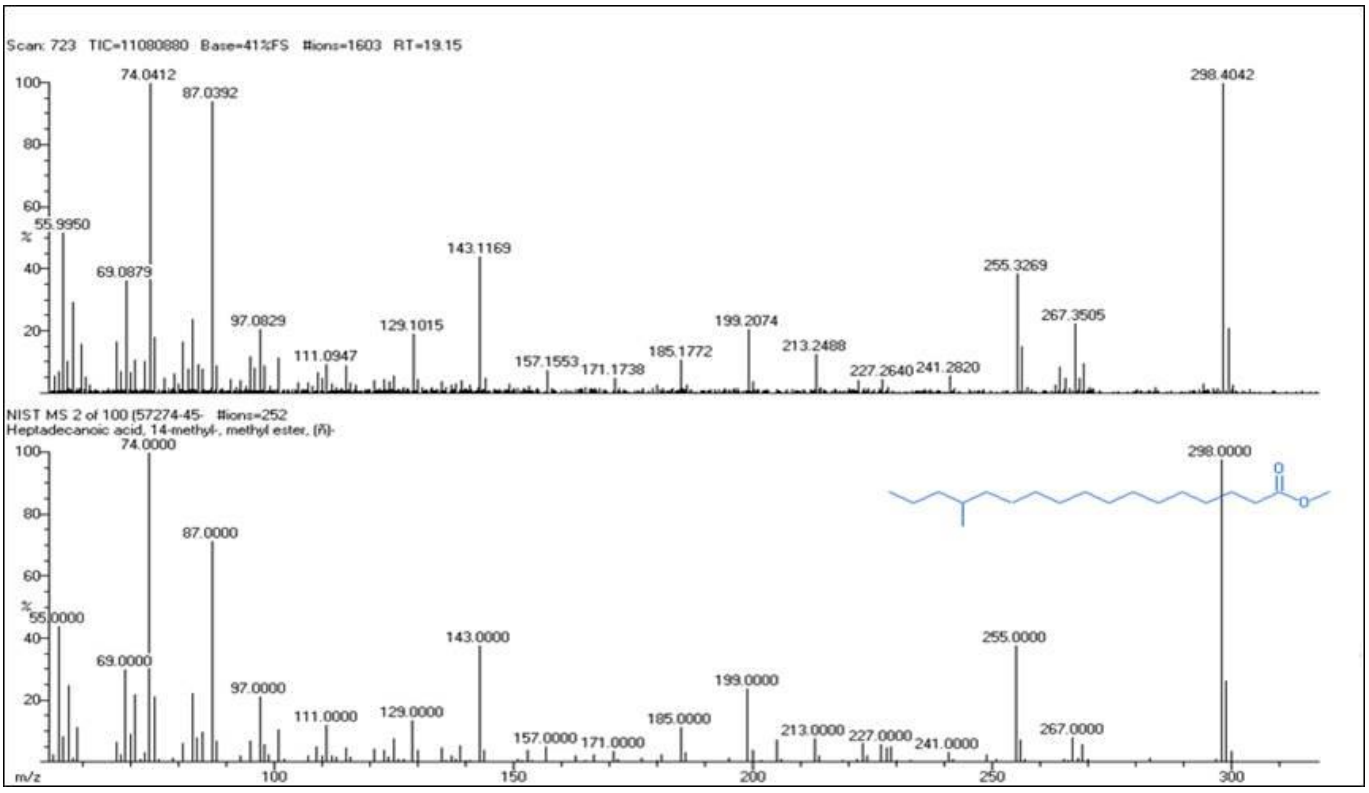

Figure 1. GC-MS data of *C. phlomoides* plant aqueous leaves extract

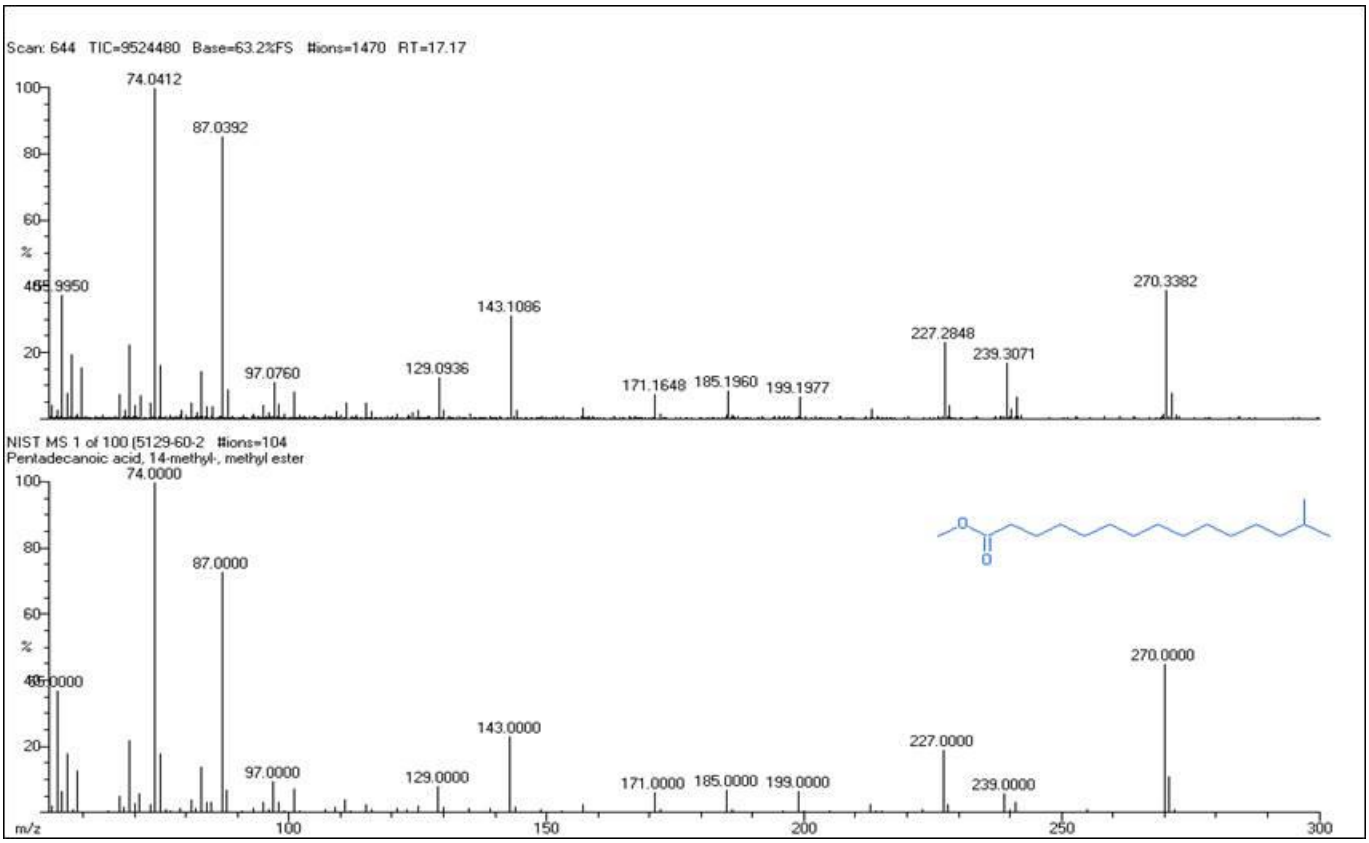

Figure 2. GC-MS data of *C. phlomoides* plant aqueous leaves extract

3.2. UV-visible analysis of AgNPs

Figure 3 reveals the UV-visible spectra of silver nanoparticles confirming that the silver nanoparticles formed at 489 nm. The synthesis of silver nanoparticles using *Peltophorum pterocarphum* plant extract was observed at the same absorption range from 390 to 490 nm. After the addition of plant extract, the colorless silver nitrate solution changed to brown color due to the biological reduction of silver nitrate into silver nanoparticles. The silver nanoparticle has free electrons giving the SPR band. The synthesized nanoparticle absorbs the SPR exactly at 489 nm and the range starts from 360-550 nm.

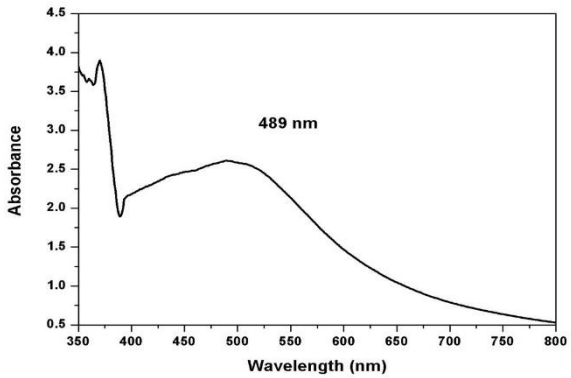

Figure 3. UV-visible spectroscopy analysis of silver nanoparticles

3.3. Fourier-transform infrared analysis of AgNPs

Figure 4 revealed the FTIR spectra of plant extract and silver nanoparticles. FTIR reported the bioactive macromolecules from the plant extract responsible for capping and stabilizing the silver nanoparticle improving their bioactive anticancer potential. **Figure 4A** shows the notable peaks at 3922, 3479, 2097,

and 1639 cm^{-1}. The peaks at 3479 and 1639 cm^{-1} represent the N-H stretching and bending vibration through amines from the proteins and other bioactive compounds of the plant extracts. The peak at 1639 cm^{-1} was observed in plant extract for the presence of NH_2 groups in amino acid. The presence of O-H stretching was noted at the peak of 3922 cm^{-1}. When comparing both FTIR spectra of plant extract and silver nanoparticles, the shift at higher ranges was seen. The polyphenols compounds of the plant are the source of OH groups and are responsible for the reduction of silver ions. This type of shift leads to the bind silver ion with free–NH groups in plant extract resulting in the stabilization of silver nanoparticles [18]. The predominant peaks in FTIR spectra were 1639-1642 cm^{-1} (protein groups), 2097-2103 cm^{-1}, and 3479-3516 cm^{-1} (amide I group). The peak at 2071 cm^{-1} shows the C-H stretching in the aldehyde group.

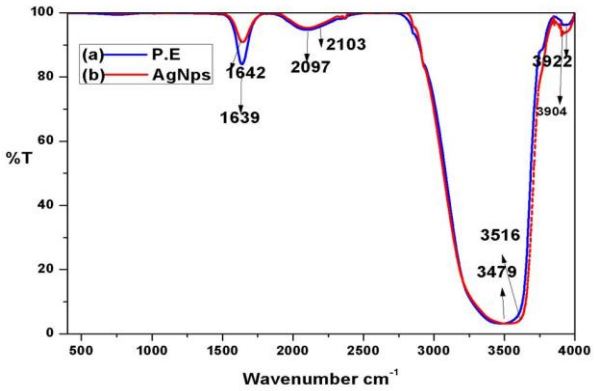

Figure 4. FTIR spectra of (a) Plant leaf extract and (b) Silver Nanoparticles

3.4. Scanning electron microscopy analysis

Figure 5 represents the structure and morphology of the green-synthesized AgNPs in SEM with energy dispersive X-ray (EDX) analysis. The spherical and ovoid structure of AgNPs was observed in the SEM micrograph. The elemental composition of green-synthesized AgNPs was observed from the EDX analysis. The yield of AgNPs was found to be 28.7%. When compared to Ag and O, the presence of other elements such as C and N were found to be present in a negligible amount. The composition of C and N present in the EDX analysis was low as compared to Ag and O, hence it could not be shown. **Table 3** shows the elemental composition of silver nanoparticles. The presence of oxygen in nanoparticles confirmed that a portion of silver was oxidized into silver oxide.

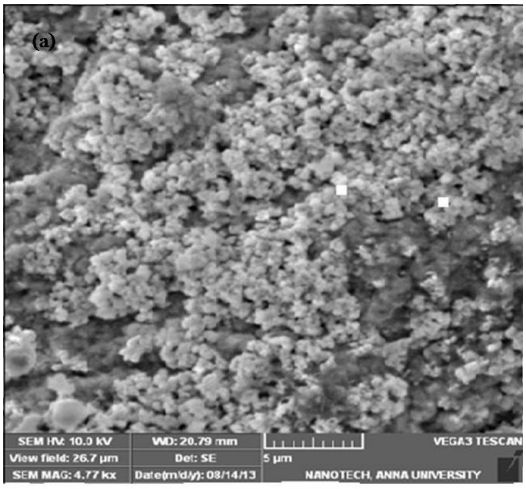

Figure 5. SEM image of green synthesized silver nanoparticles

Table 3. Quantitative analysis of AgNPs

Element	Net count	Weight %	Atom %
O	4462	29.06	73.42
Ag	29051	70.94	26.58
Total		100.00	100.00

3.5. Transmission electron studies:

Figure 6 shows the particle size varying from 25 to 100 nm. The aggregated nanoparticles cause size variation and wide size distribution. TEM reveals nanoparticles are well separated and aggregated. The shape of AgNPs was a sphere and predicted good interaction with cancerous cells due to larger surface volume area as compared to other shapes. As a result, the secondary metabolites on the surface of the AgNPs can penetrate the cancer cells of the liver and produce anticancer activity against the cancerous cell. The smaller particles (< 100 nm) produce more cytotoxic in cancerous cells than larger particles (> 100 nm) and penetrate the cell nucleus more effectively.

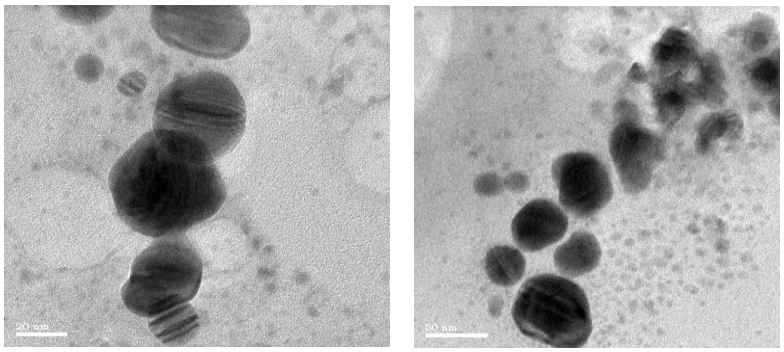

Figure 6. TEM images of silver nanoparticles

3.6. X-ray diffraction analysis

Figure 7 shows the XRD spectra of silver nanoparticles confirming that the nanoparticles were crystalline. The 2θ values were found to be 27.9°, 32.8°, 38.14°, and 46.2°, which corresponds to (220), (311), (111), and (100) planes of pure silver and coincides with ICDD (International Center for Diffraction Data) file No.01-1167. Fewer intensity peaks were observed in the area other than AgNPs, which may be due to the presence of biomacromolecules in an aqueous extract of *C. phlomoides.* Similar XRD results were previously reported for green synthesized silver nanoparticles with face-centered cubic (FCC) structure [18]. From the XRD value, it could be confirmed that the crystalline silver nanoparticles were effectively bio-reduced by *C. phlomoides* plant extract.

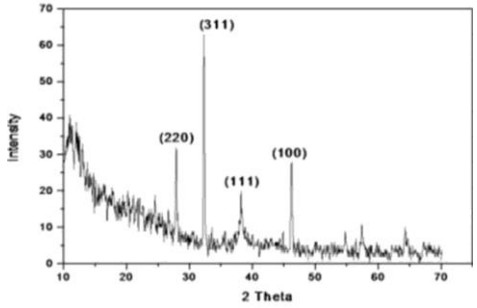

Figure 7. XRD spectra of silver nanoparticles

3.7. Dynamic light scattering and zeta potential analysis

Figure 8 shows the zeta potential for biologically reduced AgNPs. The zeta potential values range between +25 mV and -25 mV confirming highly stable nanoparticles that are highly pH and electrolyte concentration dependent. In the present investigation, AgNPs showed a negative zeta potential value and were found to be -6.02 mV and stable. The maximum particle size distribution falls in the range of 100 nm and next the aggregated particle distribution shows high in the figure of size distribution by density.

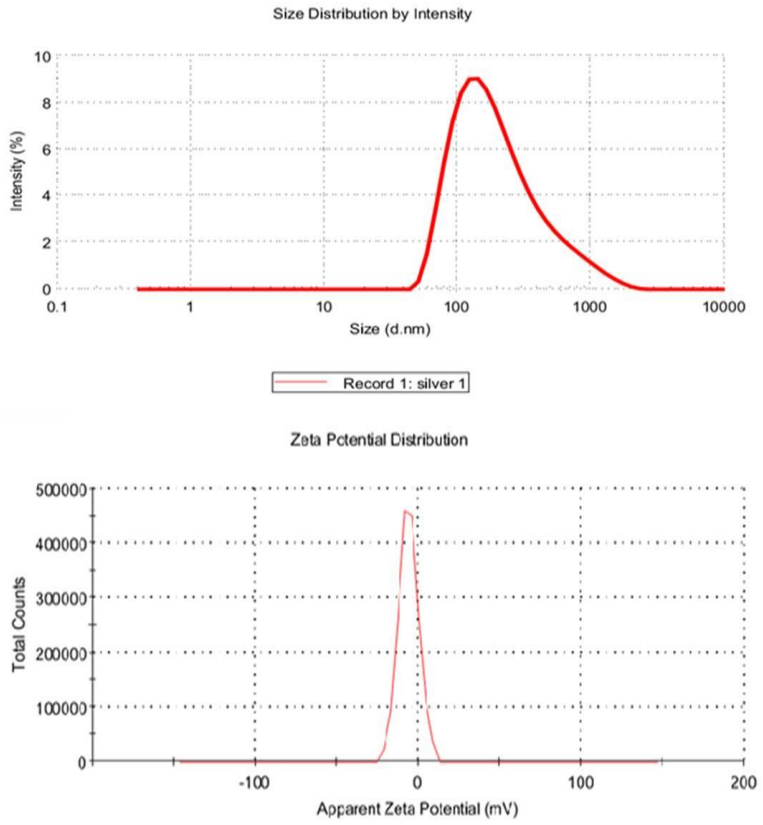

Figure 8. Size distribution of silver nanoparticles

3.8. Biochemical *in vivo* studies

In the biochemical studies, the therapeutic performance of the silver nanoparticle was evaluated and also compared with other metallic nanoparticles such as palladium and selenium nanoparticles. The anticancer potential of these nanoparticles including silver nanoparticles was investigated through the enzymatic analysis via biochemical studies and antioxidant expression in the tissue after the DEN-induced rats were treated with the nanoparticles.

3.8.1. Liver pathological enzyme analysis

As shown in **Figure 9**, the serum pathophysiological enzymes like aspartate aminotransferase (AST), alkaline transferase (ALT), alkaline phosphatase (ALP), and lactate dehydrogenase (LDH) in the control and experimental rats showed no significant difference in their activity. The DEN-induced rats that were administered with AgNPs exhibited about 1.5 times higher AST enzymic activity compared to the control group 1. Similarly, other enzymes like ALT, ALP, LDH, and gamma-glutamyl transferase (γGT) were also found to be increased. It is interesting to note that the treatment of DEN-induced rats with SeNPs decreased the serum pathophysiological enzyme level: AST from 143 to 91.05 U/L, ALT from 134.02 to 90.5 U/L, ALP from 221 to 170.34 U/L, LDH from 241 to 211.5 U/L and γGT 11.05 to 7.2 U/L. In AgNPs treated

group 3 rats, comparatively decreased enzyme activity was seen: AST from 143.21 to 106.34 U/L, ALT from 134.02 to 124.58 U/L, ALP from 221 to 158 U/L, LDH from 241 to 208.43 U/L, and γGT from 11.05 to 9.23 U/L. However, in the case of PdNPs treated group 5 rats, no satisfactory results were obtained. When compared to SeNPs and AgNPs treated groups, the results were shown: AST decreased from 143 to 128 U/L, ALT from 134.02 to 128.01 U/L, ALP from 221 to 142.81 U/L, LDH from 241 to 180.32 U/L, and γGT from 11.05 to 10.42 U/L. Meanwhile, there was not much difference between the DEN-induced group 2 rats and PdNPs-treated group 5 rats. Plant extract-treated group 6 rats, did not show significant changes in their values, which as shown in **Figure 9**.

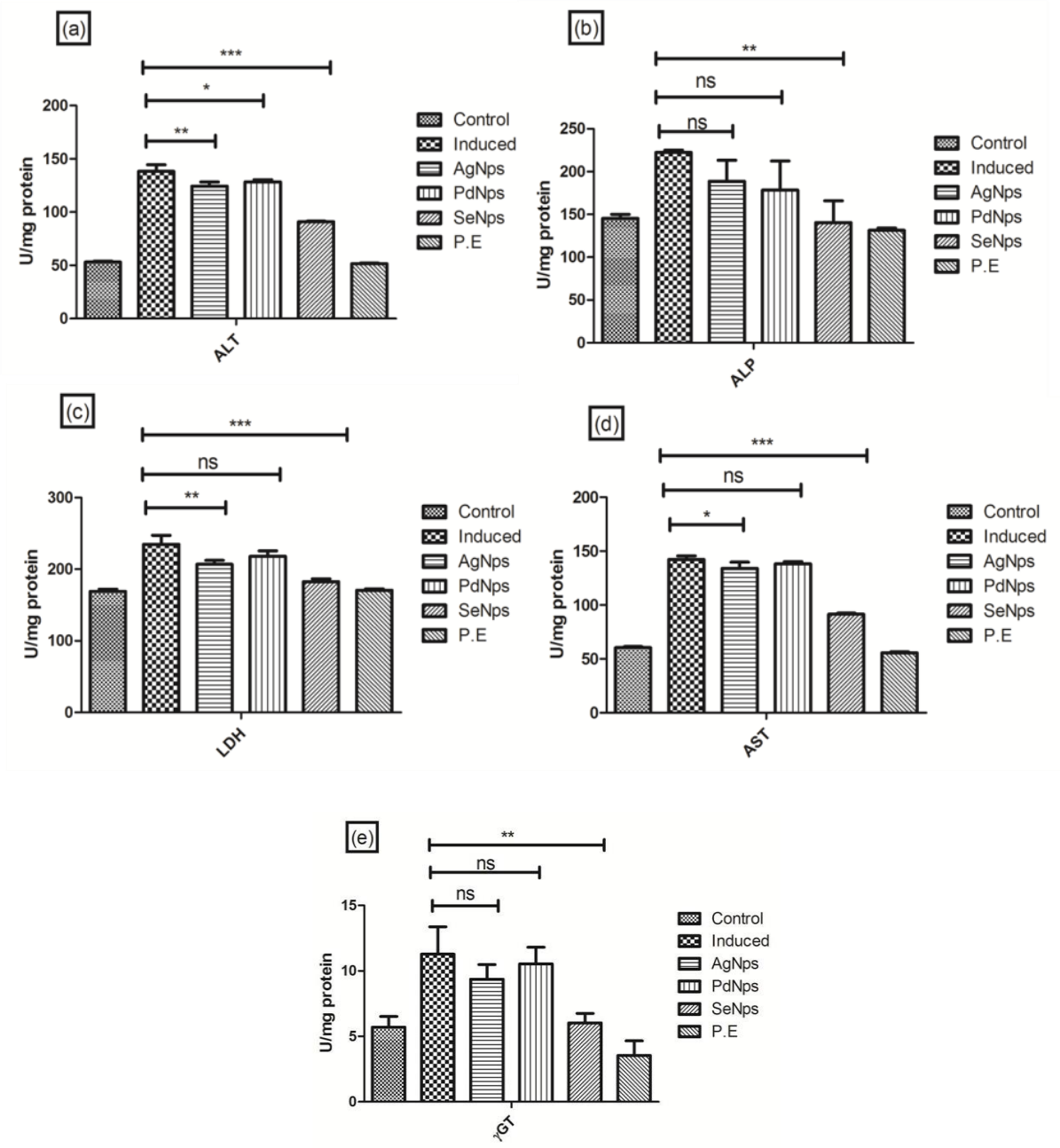

Figure 9. Effect of nanoparticles on serum liver pathological enzymes (a) ALT, (b) ALP, (c) LDH, (d) AST, and (e) γGT. Results were expressed as mean ± standard deviation (SD; n = 6). The significance when compared with the DEN-induced group of rats was shown as ns (not significant), * ($P < 0.05$),** ($P < 0.01$), and *** ($P < 0.005$).

The activities of liver pathophysiological enzymes AST, ALT, ALP, LDH, and γGT in control and experimental rats are presented in **Figure 9**. In the DEN-induced group, there was a significant increase in the activities of all of these enzymes, when compared to the control group. Among all the enzymes, the activity of ALT was found to be drastically increased (221 U/L). Since the liver is the major site for the metabolic enzymatic transformation of DEN molecule, it has been established that the unbearable production of free radicals and toxic reactive oxygen species (ROS) in hepatic cells could be the reason for oxidative stress, which ultimately leads to liver damage [19]. The disease condition pathological changes during the progression of tumors and its inhibition by chemopreventive agents are supposed to be revealed in the biochemical analysis and histopathological studies of the host tumor residing system. Even though there are so many macromolecules, most of the enzymes would leak from the damaged organ tissues, and enzymes are discharged into the body fluids depending on their tissue specificity and catalytic activity. Thus, the study of marker enzymes in serum and tissues is more important in the evaluation of respective tissue damage. Usually, the serum enzymes including transaminases (AST and ALT), LDH, ALP, and GGT denote the phase and function of the liver. Among other enzymes, transaminase elevation is considered to be the most susceptible marker in the examination of hepatocellular damage and loss of membrane functional integrity [20]. Since ALT is considered a promising serum marker, the level of ALT in serum is directly related to the high risk of HCC progression in hosts with chronic hepatitis [21].

LDH is one of the cytosolic enzymes that boost up the reversible oxidation of L-lactate substrate into pyruvate product. Increased LDH activity in serum shows the impairment of hepatic tissues and cellular leakage. The amount of LDH strongly corresponds to the size of the tumor, as the rate of glycolysis takes place in cancerous conditions, which is the only energy source pathway for the tumor cells [22]. ALP is another important liver marker enzyme whose elevated levels in serum indicate diseased conditions and alterations in bile flow. It is established from many studies, that the fast-dividing cells discarded a high amount of ALP as they resided in the bile canalicular plasma membrane [23].

GGT is also considered to be an important marker of liver cancer. It is present on the exterior membrane of the liver cells. An increase in its level leads to cholestasis and bile duct necrosis [24]. Generally, the cellular glutathione homeostasis maintained by GGT and its concentration is often raised in malignancy [25]. If necrosis takes place within the tumor organ or from a nearby invaded non-tumor tissue or leakage from tumor cells, it may lead to such drastic raise of enzymes in the serum [26].

In the present study, the serum pathological enzymes were found to have increased significantly in the SeNPs-treated group which showed the effective anticancer properties of selenium nanoparticles. The proper mechanism behind the anticancer properties of nanoparticles is not well established even though the observed results revealed the anticancer properties of SeNPs against DEN-induced HCC in Swiss Wistar rats.

3.8.2. Enzymic antioxidants

From the results, it was observed that the DEN-induced rats treated with SeNPs showed an increase in the serum enzymic antioxidant level: catalase (CAT) from 18.89 to 50.02 U/L, superoxide dismutase (SOD) from 1.4 to 6.9 U/L, glutathione S-transferase (GST) from 1.77 to 15.6 U/L, glutathione peroxidase (GPx) from 5.79 to 24.79 U/L, and glutathione reductase (GR) from 3.89 to 16.58 U/L. Whereas in AgNPs treated group 3 rats, comparatively increased enzyme activity has shown: CAT from 18.89 to 45.27 U/L, SOD from 1.4 to 6.55 U/L, GST from 1.77 to 13.16 U/L, GPx from 5.79 to 20.05 U/L, and GR from 3.89 to 15.28 U/L.

PdNPs treated group 5 rats doesn't show good results as compared to SeNPs and AgNPs treated groups. While there was an increase in the enzymic antioxidant level: CAT from 18.89 to 23.35 U/L, SOD from 1.4 to 5.45U/L, GST from 1.77 to 10.05 U/L, GPx from 5.79 to 19.1 U/L, and GR from 3.89 to 12.5 U/L,

there was no considerable difference between the DEN-induced group 2 and PdNPs treated group 5 rats.

The antioxidant enzyme activities of the experimental rat groups did not exhibit any significant variation between the control and plant extract-treated rats. DEN-induced group 2 rats showed a reduction in antioxidant activities of all the enzymes as compared to the group 1 control.

Serums from the experimental animal were analyzed for their antioxidant levels in the blood. Serum enzymic antioxidants which exist in biological systems, chiefly include SOD, a type of enzymic antioxidant that breaks down the toxic superoxide anion into oxygen and hydrogen peroxide by catalyzing the reaction [27,28]; CAT, a type of antioxidant enzyme that switches hydrogen peroxide to water and oxygen using either an iron or manganese as a co-factor [29,30]; and GPx, an enzyme containing four selenium-cofactors that facilitates the conversion of hydrogen peroxide and organic hydroperoxides.

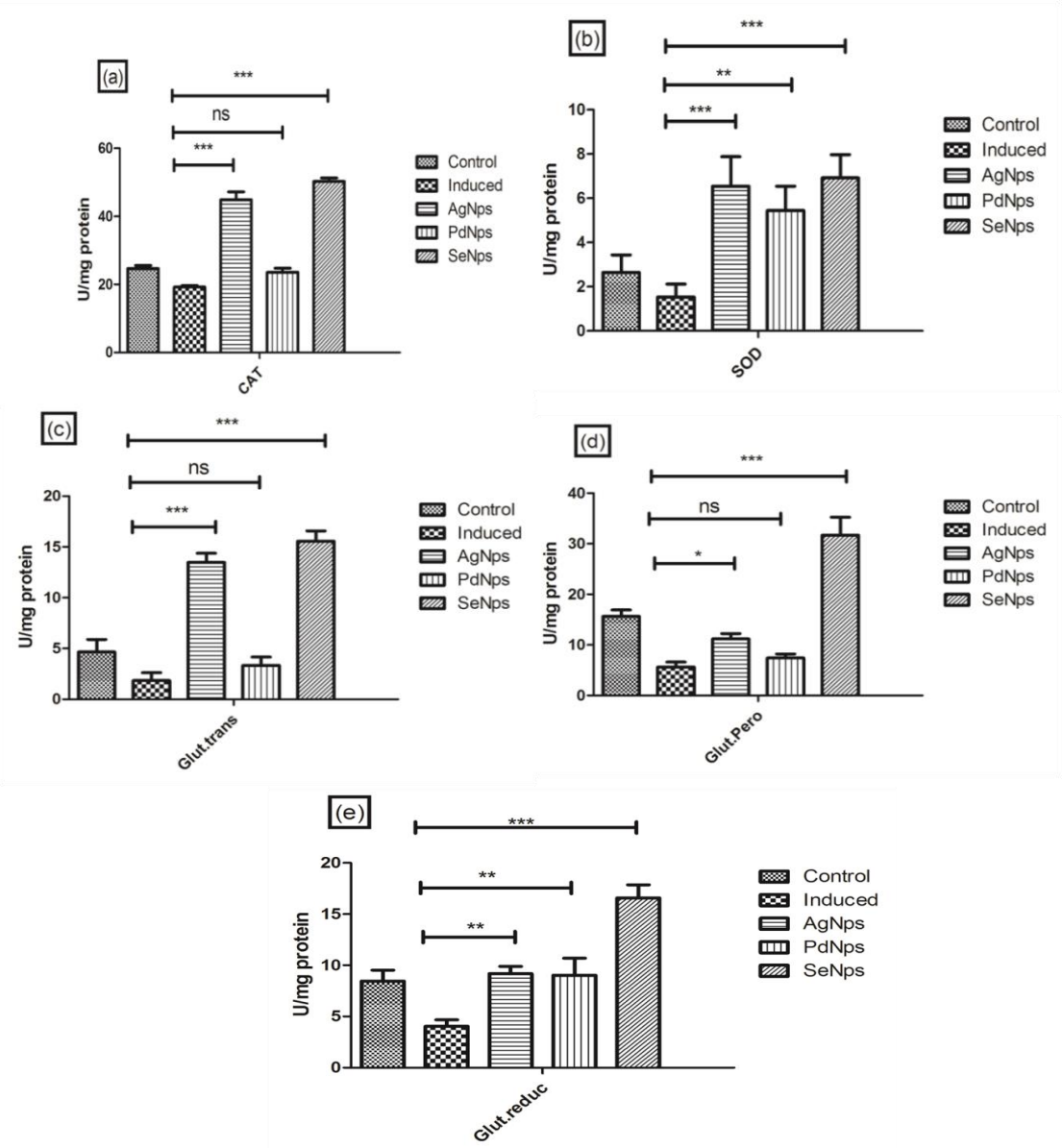

Figure 10. Effect of green synthesized metallic nanoparticles on enzymic antioxidants (a) catalase, (b) superoxide dismutase, (c) glutathione S-transferase, (d) glutathione peroxidase, and (e) glutathione reductase. Results were expressed as mean ± standard deviation (SD, n = 5). The significance when compared with the DEN-induced group of rats was shown as ns (not significant), * ($P < 0.05$),** ($P < 0.01$), and *** ($P < 0.005$).

Figure 10 reveals the effect of green synthesized metallic nanoparticles on enzymic antioxidants such as CAT, SOD, GST, GPx, and GR. Biochemical assay of SOD, CAT, and GPx is a usual step in determining the oxidative stress in a cell and the antioxidative properties of plant extracts [31]. These enzymes are estimated quantitatively to find out the progression of the tumor, the antitumor properties of herbal extracts and their derivatives, cytotoxic effect of toxic chemicals, plant extracts, and nanoparticles [32].

SOD transforms O^{2-} into oxygen and H_2O_2, but with the presence of GPx and CAT, H_2O_2 is transformed into water. In this manner, the enzymic antioxidants help to convert the cytotoxic substance in the body into harmless products [33]. These enzymic antioxidants naturally exist in the healthy body, which, however, turn downs in the case of cancer. The current results showed a significant decline in antioxidant enzyme activity (SOD, CAT, and GPx) in DEN-induced rats as compared to the control rats. However, the SeNPs treated rats showed appreciably increased levels of enzymic antioxidants to near normal. Significant reduction in the development of liver cancer progression in SeNPs oral-administered rats is proved by the reduced tumor markers and antioxidant enzyme levels. Most of the studies showed that patients who underwent chemotherapy and mastectomy for liver cancer had a drastic decrease in antioxidant levels. Hence, it is concluded that the chemotherapeutic agents generate superoxide and hydroxyl radicals during treatment which causes side effects [34-37]. The present study shows that AgNPs could be a good antioxidant supplement, chemopreventive agent, and anticancer agent which could be either due to the triggering of GPx or its highly enhanced permeability and retention (EPR) effect in the liver cancer tissue.

3.8.3. Non-enzymic antioxidant analysis

Figure 11 shows the effect of metallic nanoparticles on non-enzymic antioxidants such as vitamins A, E, and C. Non-enzymic antioxidants assay of vitamins A, E, and C provides protection mechanisms through GSH by GPx, along with vitamin A acting as a co-substrate to detoxify H_2O_2 and to make the free radicals harmless. The non-enzymic antioxidant activity changes of control and experimental rat groups have shown in **Figure 11**. GSH and vitamin A, the potent intracellular antioxidants, defend the cells from ROS damage [38]. Vitamin A is a type of fat-soluble vitamin, which is very important for the growth, maintenance, and duplication of epithelial cells. Vitamin A splits the lipid peroxide (LPO) chain in the cell membrane and prevents its formation. Vitamin A is a great toxic free radical scavenger (O^{-}) and a chain-breaking antioxidant. Among all the other functions, the most important function of Vitamin A is free radical scavenging, which protects the cells from oxidative damage [39]. Raghavan & Kumari studied that *Terminalia arjuna* EtOH extract on alloxan-induced diabetic rats showed a significant increase in SOD, CAT, GPx, GST, GR, GSH, vitamin A, vitamin C, and vitamin E [40]. Gurunagarajan & Pemaiah also established a gradual elevation in vitamin A level, when mice were treated with *Leonotis nepetifolia* EtOH crude extract against EAC cells [41]. When berberine type of an isoquinoline alkaloid is administered against 7,12-dimethylbenz(a)anthracene-induced skin carcinogenesis, it significantly boosted the activities of enzymatic antioxidants as well as nonenzymatic antioxidants including SOD, CAT, GPx, GSH, and vitamin A by which free radicals and lipid peroxidation were reduced [41]. *Ammannia baccifera* significantly reduced the rate of LPO and increased the behavior of enzymic (SOD, CAT, GSH), non-enzymic (vitamins A and D) antioxidants in Dalton's lymphoma ascites (DLA) bearing Swiss albino mice [42]. A significant decrease in vitamins C and E and GSH in DLA-bearing mice could be due to the generation of scavenged free radicals and the products of lipid peroxidation caused by the tumor effect.

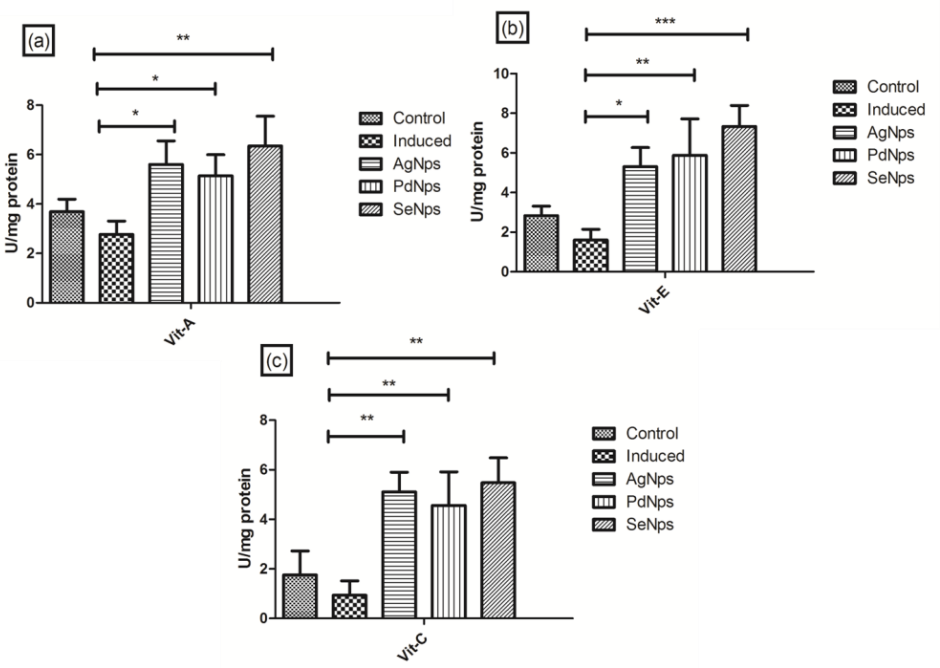

Figure 11. Effect of green synthesized metallic nanoparticles on non-enzymic antioxidants (a) vitamin A, (b) vitamin E, and (c) vitamin C. Results were expressed as mean ± standard deviation SD (n=6). The significance when compared with the DEN-induced group of rats was shown as * ($P < 0.05$),** ($P < 0.01$), and *** ($P < 0.005$).

Vitamin E protects the body from toxic free radicals, which otherwise leads to aging, a process in which oxygen and other free radicals break down the normal body's tissues. It helps to neutralize or scavenge the free radicals, which naturally exist as unstable molecules, hence saving our body from free radical damage by accepting/donating electrons from free radicals to balance themselves. When a saturated amount of vitamin E is present in the living body, unbalanced free toxic radicals accept their electrons from vitamin E molecules and leave the healthy molecules alone, causing comparatively less damage to the tissues [43]. Lower levels of vitamins E and C have been indicated in the DEN-induced rat serum when compared with the control rat, which is due to the high oxidative stress. Tumor growth might also have contributed to the low levels of vitamins E and C.

When oxidative stress is present, it has been found that ascorbic acid is in oxidized form in the body. The change in ascorbic acid level is directly proportional to the level of vitamin E, as a sufficient amount of ascorbic acid is required for the regeneration of vitamin E, an aqueous antioxidant that requires GSH [44]. Since vitamins C and E are synergistic antioxidants, the administration of plant extract and SeNPs significantly improved the vitamin E level in the liver of DEN-induced group 4 rats. The results obtained were found to be similar to a previous study [45], where the levels of non-enzymic antioxidants (vitamins A and E) were significantly enhanced in Swiss albino rats when treated with a protein fraction of *Cynodon dactylon* leaf. The GPx level was found to be decreased from 1 to 6.42 U/mg of protein in DEN-induced rats as compared to the other groups. Nami-A [Imidazoliumtrans-tetrachloro(dimethylsulfoxide)imidazoleruthenium(III)]-loaded NPs demonstrated the greater antitumor effect by inhibiting metastatic tumor growth in T739 mice, both *in-vitro* and *in-vivo* [46].

Vitamin C retains natural antioxidant defense, helping out to inhibit LPO production. Since vitamin C is an electron donor, otherwise called a reducing agent and antioxidant, it prevents other substances from getting oxidized [12]. Vitamin C is an exceptional hydrophilic antioxidant, and it voluntarily scavenges ROS and peroxyl radicals [47]. It also acts as a co-antioxidant, by regenerating vitamins A and E, and GSH from free radicals. It was observed that a decreased level of vitamin C is present in the liver of DEN-bearing rats.

This decreased level could be caused by the increased utilization of vitamin C in deactivating the increased level of ROS or to decrease the GSH level [48]. The administration of AgNPs improved the level of vitamin C in the liver of DEN-induced rats, which is expected to increase the GSH level or trigger the system to recycle the dehydro-ascorbic acid back to ascorbic acid. The level of non-enzymic antioxidant status declined in liver cancer-bearing animals [49], and the present study also correlates with the existing results. It might be due to the overutilization of these antioxidants to scavenge toxic free radicals. The simultaneous administration of SeNPs reversed the changes induced by DEN carcinogen exposure to near normal, and these data support the hypothesis that SeNPs are effective chemopreventive agents.

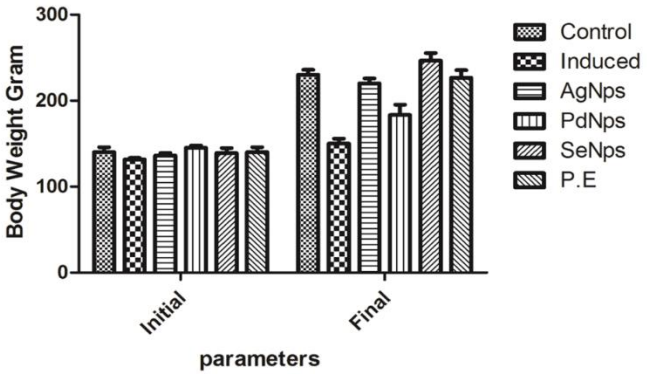

Figure 12. Effect of metallic nanoparticles on body weight of experimental rats. Results of all the groups were expressed as mean ± standard error of the mean (SEM; n = 6), where the $P < 0.005$.

Figure 12 reveals the effect of metallic nanoparticles on the body weight of experimental rats. The anticancer efficacy of green synthesized metal nanoparticles against DEN-induced HCC was studied in male Wistar albino rats. **Figure 12** showed the changes in body weight, before and after treatment, for controlled and experimental rats. The initial rats' body weight of 190 g increased gradually up to 230 g in all the experimental groups. During treatment, the body weight of the experimental groups decreased step by step with visible hair loss on the skin which might be due to the impairment of hepatic cells accordingly with chemical induction of DEN, whereas the control group rats remained the same weight. At the final stage of the experiment, the body weight of control group 1 rats (250 g) did not show any weight loss, but the weight of DEN-induced group 2 rats drastically decreased to 180 g. As compared to the group 2 rats, the AgNPs-treated group 3 rats showed relatively improved body weight (200 g). However, no significant changes in body weight were observed in the palladium nanoparticles treated group 5 rats, which showed almost the same weight as group 2 rats, and decreased when compared to group 3 rats. HCC is a highly malignant cancer that has high morbidity and mortality rate and a poor prognosis. It is highly resistant to chemotherapeutic agents [50], and is associated with distinct symptoms of weight loss and tissue wasting [51]. A quick loss in body weight can be observed in HCC-bearing animals.

4. Conclusion

The present investigation reveals that the biosynthesis of silver nanoparticles was achieved with an aqueous extract of leaves from the *Clerodendron phlomoides* plant. The size and shape of the biosynthesized silver nanoparticle range from 25 to 100 nm, and are spherical for the potential to interact with the cancerous cell in the liver of Wister rats. During the biosynthesis process, the secondary metabolites reduce the silver nitrate solution to silver nanoparticles and coat the nanoparticles with secondary metabolites of the plant extract into a potential drug delivery vehicle to cancer cells. The XRD investigation of the AgNPs confirmed the nanoparticles are crystalline and the DLS studies revealed that the size of the AgNPs varies

from 50 to 100 nm. Due to the aggregation of nanoparticles, the size of the aggregates shows higher and particles are stable in negative potential. The anticancer potential of AgNPs was evaluated in DEN-induced liver cancer in Wister Rats, where the biochemical studies of the anticancer potential via enzymatic analysis and anti-oxidants were carried out. Additionally, AgNPs have a considerable chemoprevention potential when compared with other metallic nanoparticles. In summary, the biosynthetic process of AgNPs is an eco-friendly process for metallic nanoparticle synthesis and a good drug delivery vehicle for the treatment of liver cancer.

Disclosure statement

The authors declare no conflict of interest.

References

[1] Kiernan F, 1833, XXIX. The Anatomy and Physiology of the Liver. Philos Trans R Soc, 123: 711–770.

[2] Nelson DR, 2009, The Cytochrome P450 Homepage. Hum Genomics, 4(1): 59.

[3] Liu CY, Chen KF, Chen PJ, 2015, Treatment of Liver Cancer. Cold Spring Harb Prespect Med, 5(9): a021535.

[4] Rajeshkumar S, 2016, Anticancer Activity of Eco-Friendly Gold Nanoparticles Against Lung and Liver Cancer Cells. J Genet Eng Biotechnol, 14(1): 195–202.

[5] Evans ER, Bugga P, Asthana V, et al, 2018, Metallic Nanoparticles for Cancer Immunotherapy. Mater Today, 21(6): 673–685.

[6] Desai N, Momin M, Khan T, et al, 2021, Metallic Nanoparticles as Drug Delivery System for the Treatment of Cancer. Expert Opin Drug Deliv, 18(9): 1261–1290.

[7] Sharma A, Goyal AK, Rath G, 2018, Recent Advances in Metal Nanoparticles in Cancer Therapy. J Drug Target, 26(8): 617–632.

[8] Ravindran A, Chandran P, Khan SS, 2013, Biofunctionalized Silver Nanoparticles: Advances and Prospects. Colloids Surf B Biointerfaces, 105: 342–352.

[9] Rai M, Yadav A, Gade A, 2009, Silver Nanoparticles as a New Generation of Antimicrobials. Biotechnol Adv, 27(1): 76–83.

[10] Rai M, Kon K, Ingle A, et al, 2014, Broad-Spectrum Bioactivities of Silver Nanoparticles: the Emerging Trends and Future Prospects. Appl Microbiol Biotechnol, 98(5): 1951–1961.

[11] Durán N, Durán M, De Jesus MB, et al, 2016, Silver Nanoparticles: a New View on Mechanistic Aspects on Antimicrobial Activity. Nanomedicine, 12(3): 789–799.

[12] Wei L, Lu J, Xu H, et al, 2015, Silver Nanoparticles: Synthesis, Properties, and Therapeutic Applications. Drug Discov Today, 20(5): 595–601.

[13] Hembram KC, Kumar R, Kandha L, et al, 2018, Therapeutic Prospective of Plant-Induced Silver Nanoparticles: Application as Antimicrobial and Anticancer Agent. Artif Cells Nanomed Biotechnol, 46(sup3): S38–S51.

[14] Saratale RG, Shin HS, Kumar G, et al, 2018, Exploiting Antidiabetic Activity of Silver Nanoparticles Synthesized Using *Punica Granatum* Leaves and Anticancer Potential Against Human Liver Cancer Cells (Hepg2). Artif Cells Nanomed Biotechnol, 46(1): 211–222.

[15] Srikar SK, Giri DD, Pal DB, et al, 2016, Green Synthesis of Silver Nanoparticles: A Review. Green Sustain Chem, 6(1): 34–56.

[16] Sriranjani R, Srinithya B, Vellingiri V, et al, 2016, Silver Nanoparticle Synthesis Using *Clerodendrum Phlomidis* Leaf Extract and Preliminary Investigation of its Antioxidant and Anticancer Activities. J Mol Liq, 220: 926–930.

[17] Lakshmi V, Bai GVS, 2016, In Vitro Anticancer Activity of *Clerodendrum Phlomidis* Leaves and Its Silver Nanoparticles on Human Breast Cancer Cell Line (MCF-7). Asian J Innov Res, 1(2): 1–5.

[18] Khalil MM, Ismail EH, El-Baghdady KZ, et al, 2014, Green Synthesis of Silver Nanoparticles Using Olive Leaf Extract and Its Antibacterial Activity. Arab J Chem, 7(6): 1131–1139.

[19] Gey KF, 1993, Prospects For The Prevention of Free Radical Disease, Regarding Cancer and Cardiovascular Disease. Br Med Bull, 49: 679–699.

[20] Plaa GL, Hewitt WR, 1989, Principle and Methodology of Toxicology, 2nd ed., Raven Press, New York.

[21] Tarao K, Takemiya S, Tamai S, et al, 1997, Relationship Between the Recurrence of Hepatocellular Carcinoma (HCC) and Serum Alanine Aminotransferase Levels in Hepatectomized Patients with Hepatitis C Virus-Associated Cirrhosis and HCC. Cancer, 79(4): 688–694.

[22] Prasad SB, Giri A, 1999, Effect of Cisplatin on The Lactate Dehydrogenase Activity and Its Isozyme Pattern in Dalton's Lymphoma Bearing Mice. Cytologia, 64(3): 259–267.

[23] Frederiks WM, Van Noorden CJ, Aronson DC, et al, 1990, Quantitative Changes in Acid Phosphatase, Alkaline Phosphatase and 5'-Nucleotidase Activity in Rat Liver After Experimentally Induced Cholestasis. Liver, 10(3): 158–166.

[24] Bulle F, Mavier P, Zafrani ES, et al, 1990, Mechanism of Γ-Glutamyl Transpeptidase Release in Serum During Intrahepatic and Extrahepatic Cholestasis in The Rat: a Histochemical, Biochemical and Molecular Approach. Hepatology, 11(4): 545–550.

[25] Daubeuf SP, Leroy A, Paolicchi A, et al, 2002, Enhanced Resistance of HELA Cells to Cisplatin by Overexpression of Gamma-Glutamyl Transferase. Biochem Pharmacol, 64(2): 207–216.

[26] Schwartz MA, West M, Walsch WS, et al, 1962, Serum Enzymes in Disease. VIII. Glycolytic and Oxidative Enzymes and Transaminases in Patients With Gastrointestinal Carcinoma. Cancer, 15(2): 346–353.

[27] Bannister JV, Bannister WH, Rotilio G, 1987, Aspects of the Structure, Function, and Applications Of Superoxide Dismutase. CRC Crit Rev Biochem, 22(2): 111–180.

[28] Zelko IN, Mariani TJ, Folz RJ, 2002, Superoxide Dismutase Multigene Family: a Comparison of the CuZn-SOD (SOD1), Mn-SOD (SOD2), and EC-SOD (SOD3) Gene Structures, Evolution, and Expression. Free Radic Biol Med, 33(3): 337–349.

[29] Chelikani P, Fita I, Loewen PC, 2004, Diversity of Structures and Properties Among Catalases. Cell Mol Life Sci, 61(2): 192–208.

[30] Zámocký M, Koller F, 1999, Understanding the Structure and Function of Catalases: Clues from Molecular Evolution and in Vitromutagenesis. Prog Biophys Mol Biol, 72(1): 19–66.

[31] Siddiqui IA, Raisuddin S, Shukla Y, 2005, Protective Effects of Black Tea Extract on Testosterone Induced Oxidative Damage in Prostate. Cancer Lett, 227(2): 125–132

[32] Cragg GM, Grothaus PG, Newman DJ, 2009, Impact of Natural Products on Developing New Anticancer Agents. Chem Rev, 109(7): 3012–3043.

[33] Ray G, Husain SA, 2002, Oxidants, Antioxidants and Carcinogenesis. Indian J Exp Biol, 40(11): 1213–1232.

[34] Lipinski B, 2011, Hydroxyl Radical and Its Scavengers in Health and Disease. Oxid Med Cell

Longev, 2011:809696.

[35] Zou Z, Chang H, Li H, et al, 2017, Induction of Reactive Oxygen Species: an Emerging Approach for Cancer Therapy. Apoptosis, 22(11): 1321–1335.

[36] Tas F, Hansel H, Belce A, et al, 2005, Oxidative Stress in Breast Cancer. Med Oncol, 22(1): 11–15.

[37] Singh G, Maulik SK, Jaiswal A, et al, 2010, Effect on Antioxidant Levels in Patients of Breast Carcinoma During Neoadjuvant Chemotherapy and Mastectomy. Malays J Med Sci, 17(2): 24–28.

[38] Circu ML, Moyer MP, Harrison L, et al, 2009, Contribution of Glutathione Status to Oxidant Induced Mitochondrial DNA Damage in Colonic Epithelial Cells. Free Radic Biol Med, 47(8): 1190–1198.

[39] Raghavan B, Kumari SK, 2006, Effect of Terminalia Arjuna Stem Bark on Antioxidant Status in Liver and Kidney of Alloxan Diabetic Rats. Indian J Physiol Pharmacol, 50(2): 133–142.

[40] Gurunagarajan S, Pemaiah B, 2010, Anti-Tumor and Antioxidant Potentials of Ethanolic Extract of *Leonotis Nepetefolia R.Br.* Against Ehrlich Ascites Carcinoma Cell Lines. J Pharm Res, 3(12): 2990–2992.

[41] Manoharan S, Vasanthaselvan M, Silvan S, et al, 2010, Carnosic Acid: a Potent Chemopreventive Agent Against Oral Carcinogenesis. Chem Biol Interact, 188(3): 616–622.

[42] Loganayaki N, Manian S, 2012, Antitumor Activity of the Methanolic Extract of *Ammannia Baccifera L.* Against Dalton's Ascites Lymphoma Induced Ascitic and Solid Tumors in Mice. J Ethnopharmacology, 142(1): 305–309.

[43] Traber MG, Atkinson J, 2007, Vitamin E, Antioxidant And Nothing More. Free Radic Biol Med, 43(1): 4–15.

[44] Sies H, Stahl W, 1995, Vitamins E and C, Beta-Carotene, and Other Carotenoids as Antioxidants. Am J Clin Nutr, 62(6 Suppl): 1315S–1321S.

[45] Ashokkumar K, Selvaraj K, Muthukrishnan SD, 2013, *Cynodon Dactylon* (L.) Pers.: an Updated Review of Its Phytochemistry and Pharmacology. J Med Plants Res, 7(48): 3477–3483.

[46] Chiniadis L, Giastas P, Bratsos I, et al, 2021, Insights into the Protein Ruthenation Mechanism by Antimetastatic Metallodrugs: High-Resolution X-Ray Structures of the Adduct Formed between Hen Egg-White Lysozyme and NAMI-A at Various Time Points. Inorg Chem, 60(14): 10729–10737.

[47] Packer L, Tritschler HJ, Wessel K, 1997, Neuroprotection by the Metabolic Antioxidant Alpha-Lipoic Acid. Free Radic Biol Med, 22(1-2): 359–378.

[48] Chatterjee IB, Nandi A, 1991, Ascorbic Acid: a Scavenger of Oxyradicals. Indian J Biochem Biophys, 28(4): 233–236.

[49] Thirunavukkarasu C, Prince Vijeya Singh J, Thangavel M, et al, 2002, Dietary Influence of Selenium on the Incidence of N-Nitrosodiethylamine-Induced Hepatoma with Reference to Drug and Glutathione Metabolizing Enzymes. Cell Biochem Function, 20(4): 347–356.

[50] Alsowmely AM, Hodgson HJF, 2002, Non-Surgical Treatment of Hepatocellular Carcinoma. Aliment Pharmacol Ther, 16(1): 1–15.

[51] Suriawinata AA, Thung SN, 2002, Malignant Liver Tumors. Clin Liver Dis, 6(2): 527–554.